# On the Use of Ocean Dynamic Temperature for Hurricane Intensity Forecasting

KARTHIK BALAGURU

*Marine Sciences Laboratory, Pacific Northwest National Laboratory, Seattle, Washington*

GREGORY R. FOLTZ

*Physical Oceanography Division, Atlantic Oceanographic and Meteorological Laboratory, Miami, Florida*

L. RUBY LEUNG AND SAMSON M. HAGOS

*Atmospheric Sciences and Global Change Division, Pacific Northwest National Laboratory, Richland, Washington*

DAVID R. JUDI

*Earth Systems Science, Pacific Northwest National Laboratory, Richland, Washington*

(Manuscript received 25 September 2017, in final form 29 January 2018)

ABSTRACT

Sea surface temperature (SST) and tropical cyclone heat potential (TCHP) are metrics used to incorporate the ocean's influence on hurricane intensification into the National Hurricane Center's Statistical Hurricane Intensity Prediction Scheme (SHIPS). While both SST and TCHP serve as useful measures of the upper-ocean heat content, they do not accurately represent ocean stratification effects. Here, it is shown that replacing SST within the SHIPS framework with a dynamic temperature $T_{dy}$, which accounts for the oceanic negative feedback to the hurricane's intensity arising from storm-induced vertical mixing and sea surface cooling, improves the model performance. While the model with SST and TCHP explains about 41% of the variance in 36-h intensity changes, replacing SST with $T_{dy}$ increases the variance explained to nearly 44%. These results suggest that representation of the oceanic feedback, even through relatively simple formulations such as $T_{dy}$, may improve the performance of statistical hurricane intensity prediction models such as SHIPS.

## 1. Introduction

Annually, hurricanes cause substantial damages to life and property in the global tropics and subtropics, including the United States (Emanuel 2003; Pielke et al. 2008). Thus, improving the accuracy of hurricane forecasts is extremely important from a societal standpoint. While significant progress has been made over the past few decades in hurricane track forecasting, improvements to hurricane intensity forecasts have been relatively modest (Rappaport et al. 2012), with intensity forecast errors decreasing at a rate that is between a third and a half of the rate at which track forecast errors are being reduced (DeMaria et al. 2014).

Hurricanes intensify by extracting heat energy from the ocean's surface, with the thermal disequilibrium at the air–sea interface playing a critical role (Emanuel 1986, 1999). The intense winds of hurricanes cause tremendous vertical mixing of the upper ocean and sea surface cooling, which acts as a negative feedback on the storm's intensity (Price 1981; Bender and Ginis 2000; Lin et al. 2005; D'Asaro et al. 2007; Lloyd and Vecchi 2011; Balaguru et al. 2012b). In the Statistical Hurricane Intensity Prediction Scheme (SHIPS; DeMaria and Kaplan 1994b, 1999; DeMaria et al. 2005), the statistical–dynamical hurricane intensity prediction model of NHC, the impact of the ocean on hurricane intensification is included primarily through the sea surface temperature (SST)-based potential intensity (PI) and the tropical cyclone heat potential (TCHP), which is the integral of the temperature from the surface to the depth of the 26°C isotherm (Leipper and Volgenau 1972; Goni and Trinanes 2003; Mainelli et al. 2008; Shay and Brewster 2010). Using SST assumes no mixing of the upper ocean by the storm and no negative feedback from the ocean. On the other hand, while TCHP includes ocean stratification

*Corresponding author*: Karthik Balaguru, karthik.balaguru@pnnl.gov

DOI: 10.1175/WAF-D-17-0143.1

TABLE 1. Various datasets used in our study and their sources.

| Dataset | Source |
|---|---|
| SODA (version 3.3.1) subsurface oceanic temperature profiles | https://www.atmos.umd.edu/~ocean/ |
| EN4 (version 4.2.0) subsurface oceanic temperature profiles | http://www.metoffice.gov.uk/hadobs/en4/ |
| NCEP–DOE R-2 atmospheric winds and temperature | https://www.esrl.noaa.gov/psd/data/gridded/data.ncep.reanalysis2.html |
| HURDAT2 hurricane track data | http://www.aoml.noaa.gov/hrd/hurdat/Data_Storm.html |
| Remote Sensing Systems microwave SST | http://www.remss.com |

effects to an extent, not every hurricane stirs the ocean to the depth of the 26°C isotherm. This is because the depth to which a hurricane mixes the ocean varies dynamically, depending on its current state and prevailing ocean conditions (Price 2009; Balaguru et al. 2015).

Recently, representing the ocean feedback in PI (Emanuel 1986, 1999) was shown to improve its ability to predict hurricane intensification (Lin et al. 2013; Balaguru et al. 2015). This was done by replacing SST in PI with dynamic temperature $T_{\mathrm{dy}}$, the true SST felt by the storm (Balaguru et al. 2015). The value of using an ocean-coupling PI for prediction of rapid intensification of tropical cyclones in the western Pacific was demonstrated using a decision tree model (Gao et al. 2016), but a similar technique has not been attempted within the SHIPS framework. In this study, we replace SST with $T_{\mathrm{dy}}$ in the PI formulation and estimate the impact on the predictive capability of the SHIPS framework. The layout of the paper is as follows. In section 2, we describe the data, model, and methods. The results are presented in section 3, and their implications are discussed in section 4.

## 2. Data, model, and methods

### a. Data

We use Simple Ocean Data Assimilation (SODA, version 3.3.1) 5-day mean oceanic subsurface temperature profiles, available at 0.5° spatial resolution, to estimate the oceanic parameters in the model (Carton and Giese 2008). To validate our results based on SODA reanalysis, we also used EN4 (v 4.2.0) monthly mean subsurface temperature profiles from the Met Office Hadley Centre (Good et al. 2013). These data, available at 1° spatial resolution, were produced using an objective analysis of all available hydrographic measurements including Argo. To compute the various atmospheric parameters in the model, we obtained 6-hourly winds and air temperature from the NCEP–DOE AMIP-II reanalysis (R-2; Kanamitsu et al. 2002). Hurricane track data are obtained from the National Hurricane Center's HURDAT2 database (Landsea et al. 2015). All data are obtained for the 10-yr period of 2005–14 since subsurface ocean measurements are more reliable beginning in 2005 due to the Argo program (Roemmich et al. 2009). Daily microwave SST is obtained for the period 21–28 September 2016 and used to estimate the prestorm conditions for Hurricane Matthew. The various data are freely available for download from the sources provided in Table 1.

### b. Model and methods

In this study, we use the framework of SHIPS, the NHC's statistical–dynamical hurricane intensity prediction model. It combines climatology, persistence, and synoptic-scale environmental parameters using a multivariate regression technique to predict future hurricane intensities. We use 19 predictors, 18 from DeMaria and Kaplan (1994b) and DeMaria and Kaplan (1999), plus TCHP (Mainelli et al. 2008). The climatological and persistence predictors are longitude, Julian date, current intensity, intensity change in the previous 12 h, and zonal translation speed. The synoptic predictors are PI and its square, shear and its time tendency, shear times the sine of the latitude, relative and planetary eddy flux convergence, land area under the storm, size, temperature at 200 hPa, zonal wind at 200 hPa, relative vorticity at 850 hPa, divergence at 200 hPa, and TCHP.

Following DeMaria and Kaplan (1994a) the maximum possible intensity (MPI) is calculated as

$$\mathrm{MPI} = A + B\, e^{C(\mathrm{SST}-\mathrm{SST}_o)}, \tag{1}$$

where $A$ is 66.5 kt (1 kt = 0.51 m s$^{-1}$), $B$ is 108.5 kt, $C$ is 0.1813°C$^{-1}$, and SST$_o$ is 30°C. Using (1), the PI is then computed as

$$\mathrm{PI} = \mathrm{MPI} - \text{current intensity}. \tag{2}$$

TCHP is calculated as

$$\mathrm{TCHP} = \rho C_p \int_0^{Z26} [T(z) - 26]\, dz, \tag{3}$$

where $\rho$ is the density of seawater, $C_p$ is the specific heat capacity of seawater, $T(z)$ is the temperature of seawater as a function of depth, and Z26 is the depth of the 26°C isotherm (Shay and Brewster 2010). The $T_{\mathrm{dy}}$ is calculated as

$$T_{\mathrm{dy}} = \frac{1}{L}\int_0^L [T(z)]\,dz\,. \tag{4}$$

Here, $L$ is the vertical ocean mixing length of the hurricane and is estimated as

$$L = h + \left(\frac{2\rho u_*^3 t}{\kappa g \alpha}\right)^{1/3}, \tag{5}$$

where $h$ is the initial mixed layer depth, $u_*$ is the friction velocity, $t$ is the time of mixing, $\kappa$ is the von Kármán constant, $g$ is the acceleration due to gravity, and $\alpha$ is the rate of change of density beneath the mixed layer. The other predictors within the SHIPS framework are calculated as in DeMaria and Kaplan (1994b, 1999). Both PI and TCHP are averaged over a 4° × 4° box centered over the hurricane to account for its size. To test the model with $T_{\mathrm{dy}}$, we simply replace SST with $T_{\mathrm{dy}}$ in PI. In this study, we focus on improving SHIPS using data already available for the model. Hence, we use temperature profiles only to compute seawater density, TCHP, and $T_{\mathrm{dy}}$, setting the salinity to a constant 36 psu, which is the mean value for the Atlantic. Note that we are performing hindcasts of intensity using the observed storm tracks.

We use the Monte Carlo approach of repeated random sampling to estimate the uncertainty in model performance and to evaluate the significance of replacing SST with $T_{\mathrm{dy}}$ in the model. First, we randomly select two-thirds of the input data and train the linear regression model with those data. Next, using the trained model, we make predictions for the remaining one-third of the data and obtain the variance explained and the root-mean-square error (RMSE) for the model. This whole process is repeated 1000 times to generate 1000-value sample sets of variance explained and RMSE for the model. While the means across sample sets indicate the average values of variance explained and RMSE for each model, the standard deviations across sample sets represent uncertainties in the respective parameters. Finally, to evaluate the significance of improvement attained by replacing SST with $T_{\mathrm{dy}}$ in the model, we perform a Student's $t$ test for the difference of means between the sample sets of variance explained and RMSE for the model with SST and the model with $T_{\mathrm{dy}}$.

## 3. Results

To illustrate the potential value of $T_{\mathrm{dy}}$ for statistical intensity forecasts, we begin with the case study of Matthew, the most powerful Atlantic hurricane during the 2016 season, which attained category 5 intensity at its peak and caused substantial damages in Haiti, Cuba, the Bahamas, and along the U.S. East Coast (Stewart 2017). After forming on 28 September, Matthew went through a period of rapid intensification between 30 September and 1 October, when its intensity increased from 70 to 146 kt. Figure 1a shows that Matthew experienced favorable oceanic conditions during this phase, with SSTs well above 28°C along its track. Beginning at location 1, the rate at which Matthew intensified increased over a period of 36 h up to location 6. Beyond this point, although Matthew continued to intensify, the rate at which it intensified rapidly decreased over a period of 30 h. Further on, intensity changes for Matthew became negative, and the storm decreased in intensity.

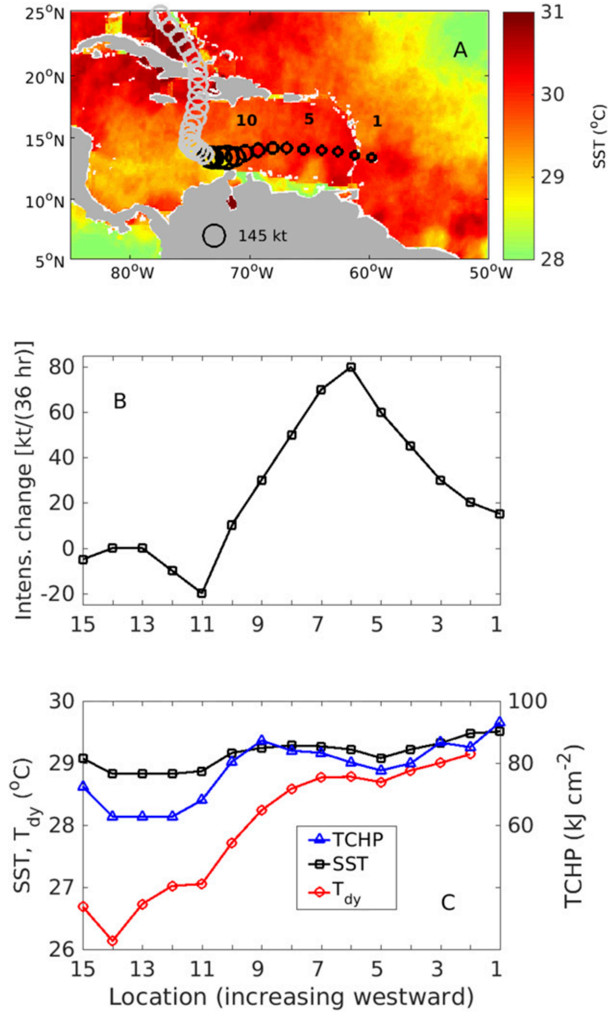


FIG. 1. (a) The track of Hurricane Matthew is indicated by circles, with prestorm SST averaged over the week before the storm in the background. (b) The 36-h intensity changes along the track of Hurricane Matthew. (c) The along-track SST, TCHP, and $T_{\mathrm{dy}}$ for Hurricane Matthew. In (b) and (c), the values are shown for the section of the track indicated in black in (a).

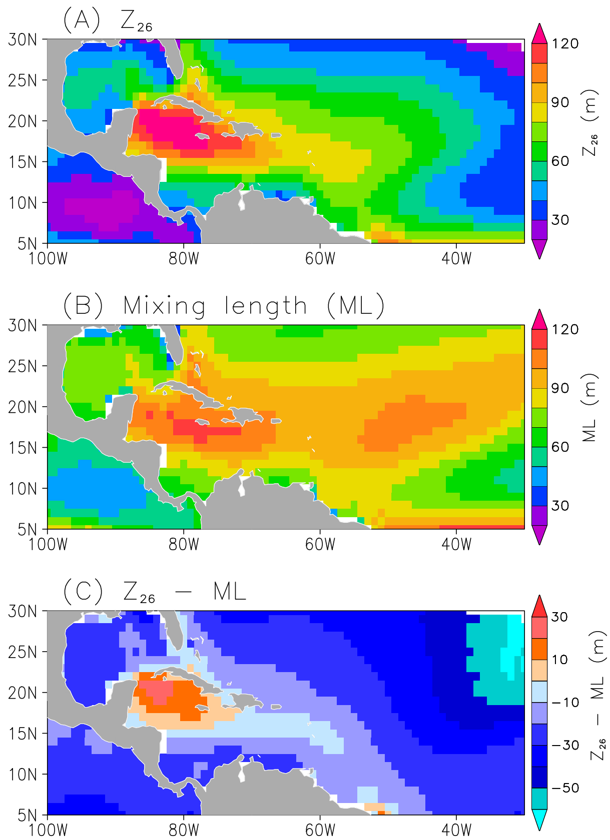


FIG. 2. Maps of climatological August–October mean (a) Z26, (b) mixing length, and (c) difference between Z26 and mixing length.

Interestingly, when considering the along-track SST and TCHP, we find that they do not vary significantly. While SST changes by about 0.5°C, variations in TCHP are below 30 kJ cm$^{-2}$. These variations in SST and TCHP are less than or comparable to their respective standard deviations (1.0°C for SST and 28.4 kJ cm$^{-2}$ for TCHP) and hence are not significant. This makes it difficult to explain the variations in Matthew's intensity using either parameter. On the other hand, the along-track $T_{dy}$ varies considerably. During the first 2 days when Matthew intensified, $T_{dy}$ remains well above 28.5°C. Subsequently, consistent with the reduction in Matthew's intensity, $T_{dy}$ decreases sharply over the next 36 h to 26°C. This drop in $T_{dy}$ of ~3°C is more than twice its standard deviation (1.2°C). During this period, the translation speed of Matthew was reduced considerably, enhancing the vertical mixing and SST cooling induced by the storm. Hence, it is possible that the better agreement of $T_{dy}$ with the storm's intensification results from its ability to account for these processes.

To understand this more generally, consider Fig. 2, which shows the climatological August–October mean thermocline depth (Z26), hurricane mixing length, and the difference between them. Figure 2a shows that Z26 is deepest in the Caribbean Sea, where it exceeds 120 m, and gradually decreases eastward. In much of the western tropical Atlantic and the Gulf of Mexico, where historically many intense hurricanes have formed, Z26 exceeds 50 m in most locations. Next, we consider the mixing length for a typical category 3 hurricane, with a wind speed of 54 m s$^{-1}$ and a translation speed of 5 m s$^{-1}$ (Fig. 2b). The mixing length exceeds 80 m in a broad area stretching from the Caribbean Sea in the west all the way into the eastern Atlantic and is punctuated by two regions where the mixing length is relatively large. The first of these two is the Caribbean Sea, where the mixing length reaches its maximum value of close to 120 m. The second region of large mixing lengths occurs approximately between 50° and 40°W and between 14° and 21°N. Here, the vertical density gradients are weak as a result of excessive evaporation and the consequent subduction (Balaguru et al. 2012a). Also, there is a region to the east of 40°W and south of 15°N where the mixing length is relatively small. Here, the thermocline is relatively shallow under the intertropical convergence zone, which enhances the upper-ocean density stratification and reduces hurricane-induced mixing. In summary, except in the Caribbean Sea, where Z26 is very large, the mixing length is usually deeper than Z26 (Fig. 2c).

We now consider the implications for predicting hurricane intensity changes. Figure 3 shows SST, TCHP, and $T_{dy}$, computed at each hurricane track location during 2005–14 and plotted against the corresponding 36-h intensity change. For all ~2100 storm locations (Figs. 3a–c), the correlations between SST, TCHP, and $T_{dy}$ and intensity change are 0.1, 0.16, and 0.19, respectively. Hence, $T_{dy}$ outperforms SST and TCHP. To understand this further, we separate track locations according to where the ocean feedback is weak ($T_{dy}$ − SST below 0.5°C) and strong ($T_{dy}$ − SST above 0.5°C). There are nearly 850 track locations where hurricane-induced SST cooling is weak. In this scenario, SST and $T_{dy}$ are both correlated at 0.08 with intensity changes, and TCHP has a higher correlation of 0.11 (Figs. 3d–f). To understand this, we consider differences in the formulations of TCHP and $T_{dy}$. If $\Delta T$ is the SST cooling, or cold wake, induced by the hurricane, then $T_{dy}$ can be written as

$$T_{dy} = \mathrm{SST} + \Delta T. \quad (6)$$

When the ocean feedback is weak, $\Delta T$ is negligible and SST is approximately equal to $T_{dy}$, causing the correlations of SST and $T_{dy}$ with intensity changes to be

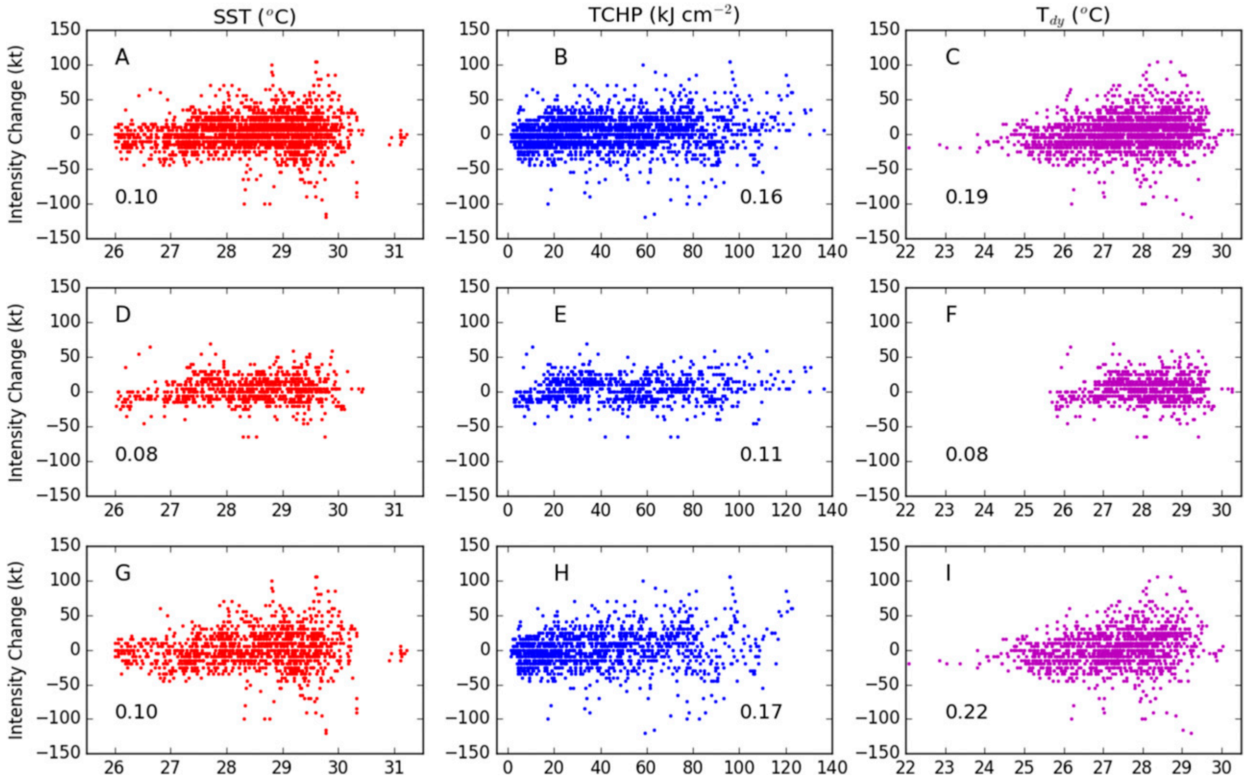

FIG. 3. Scatter between 36-h intensity changes and SST (red), TCHP (blue), and $T_{dy}$ (magenta) for the 10-yr period 2005–14. (a)–(c) All storm locations, (d)–(f) cases where the magnitude of the hurricane-induced SST cooling is below 0.5°C, and (g)–(i) cases where the cold wake magnitude is greater than 0.5°C. Correlation coefficients are also indicated in each panel.

equivalent. To explain why the correlation between TCHP and the intensity changes is higher in this case, we now consider a special situation where the mixing length equals Z26. With this simplification and using (6), the TCHP can be written as

$$\mathrm{TCHP} = \rho C_p(\mathrm{SST} - 26)\mathrm{Z26} + \rho C_p(\Delta T)\mathrm{Z26}. \quad (7)$$

Typically, the SST is well above 26°C in regions where TCHP exists. Thus, when the hurricane-induced cooling is weak, the second term on the right in (7) is negligible, and TCHP is dominated by the first term in which SST is scaled by Z26. Thus, for the same SST, a deeper thermocline will yield a considerably larger TCHP compared to a shallow thermocline. In other words, changes in SST are amplified by variations in ocean stratification, a property that tends to enhance the TCHP's correlation with intensity changes. Thus, TCHP tends to perform reasonably in regions with warm SSTs and a deep thermocline, where the ocean feedback tends to be weak (Mainelli et al. 2008; Price 2009).

Next, let us examine the situation when there is appreciable ocean feedback (Figs. 3g–i). In this case, there is a sample size of about 1250, and the correlation between the intensity changes and $T_{dy}$ is higher (0.22) than the correlation between the intensity changes and TCHP (0.17) or SST (0.1). The correlation with SST is lowest because it does not account for any ocean feedback, while the TCHP performs considerably better. However, the TCHP cannot match $T_{dy}$ for two reasons. First, the cooling of SST under a hurricane is primarily caused by vertical mixing of the upper ocean (Price 1981, 2009). Hence, a metric based on a vertical integral, such as TCHP, cannot accurately represent this effect (Price 2009). Second, the TCHP does not account for the extra cooling due to mixing below Z26. This becomes clearer when we consider the scenario in which hurricane-induced SST cooling is strong. When we subsample further using the condition that the magnitude of the cold wake is larger than 1°C, the correlation between the intensity change and TCHP is 0.1 and for $T_{dy}$ it is 0.17. This suggests that the stronger the negative feedback from the ocean, the larger the improvement is for $T_{dy}$ over TCHP. All correlations mentioned above are statistically significant at the 95% level based on a Student's $t$ test.

Having seen how $T_{dy}$ improves over SST and TCHP when used as a single predictor, we ask how the skill of

TABLE 2. Regression coefficients for various predictors in SHIPS-sst and SHIPS-tdy. Coefficients significant at the 90% level are indicated in boldface.

| Predictor | SHIPS-sst | SHIPS-tdy |
|---|---|---|
| PI | $\mathbf{5.81 \times 10^{-1}}$ | $\mathbf{1.44 \times 10^{-1}}$ |
| Shear | $\mathbf{-4.35 \times 10^{0}}$ | $\mathbf{-2.75 \times 10^{0}}$ |
| Change in intensity in the previous 12 h | $\mathbf{3.25 \times 10^{-1}}$ | $\mathbf{3.03 \times 10^{-1}}$ |
| Relative eddy flux convergence | $\mathbf{7.39 \times 10^{3}}$ | $2.25 \times 10^{3}$ |
| Planetary eddy flux convergence | $5.61 \times 10^{3}$ | $\mathbf{1.84 \times 10^{4}}$ |
| Julian day | $2.85 \times 10^{-2}$ | $\mathbf{-6.43 \times 10^{-2}}$ |
| Longitude | $7.11 \times 10^{-2}$ | $-7.33 \times 10^{-2}$ |
| Land | $\mathbf{-6.97 \times 10^{-1}}$ | $\mathbf{-7.58 \times 10^{-1}}$ |
| Size | $\mathbf{4.41 \times 10^{0}}$ | $\mathbf{3.47 \times 10^{0}}$ |
| Change in shear | $\mathbf{4.86 \times 10^{-1}}$ | $\mathbf{3.00 \times 10^{-1}}$ |
| Square of PI | $\mathbf{-3.12 \times 10^{-3}}$ | $\mathbf{-3.94 \times 10^{-3}}$ |
| Air temperature (200 hPa) | $\mathbf{-8.70 \times 10^{-1}}$ | $-4.91 \times 10^{-1}$ |
| Zonal wind (200 hPa) | $\mathbf{-3.75 \times 10^{-1}}$ | $\mathbf{-5.37 \times 10^{-1}}$ |
| Relative vorticity (850 hPa) | $-1.30 \times 10^{5}$ | $-8.25 \times 10^{4}$ |
| Shear times sine of latitude | $\mathbf{5.61 \times 10^{0}}$ | $\mathbf{1.99 \times 10^{0}}$ |
| Divergence (200 hPa) | $1.43 \times 10^{5}$ | $\mathbf{2.78 \times 10^{5}}$ |
| Zonal translational velocity | $2.43 \times 10^{-4}$ | $5.08 \times 10^{-2}$ |
| Current intensity | $\mathbf{-3.78 \times 10^{-1}}$ | $\mathbf{-8.82 \times 10^{-1}}$ |
| TCHP | $\mathbf{1.98 \times 10^{-8}}$ | $\mathbf{3.54 \times 10^{-8}}$ |
| Variance explained (%) | **40.5** | **43.9** |

the SHIPS framework changes when $T_{dy}$ is used within it. To address this, we hindcast hurricane intensity changes for the 10-yr period 2005–14 using the model and evaluate its performance with and without $T_{dy}$. We first use the model with all predictors and with PI computed using the default formula based on SST. We call this SHIPS-sst. Next, we use all the predictors similarly except we replace SST with $T_{dy}$ in MPI. We call this SHIPS-tdy. We retain TCHP in the model even when we replace SST with $T_{dy}$, since TCHP performs better than $T_{dy}$ when the ocean feedback is weak.

The variance in 36-h intensity changes explained by SHIPS-sst is 40.5% $\pm$ 2.3%, and the RMSE for the model is 18 $\pm$ 0.52 kt. These findings are comparable to results from the official SHIPS for which the variance explained is about 45%, and the RMSE is around 15 kt (DeMaria and Kaplan 1994b, 1999). The signs of the regression coefficients for the model predictors, shown in Table 2, are generally consistent with previous studies (DeMaria and Kaplan 1994b, 1999), indicating that the various predictors are acting in the right direction. If we now replace SST with $T_{dy}$ in PI, the variance explained by the model (SHIPS-tdy) increases to 43.9% $\pm$ 2.3%, and the RMSE is reduced to 17.5 $\pm$ 0.46 kt. Thus, the use of $T_{dy}$ improves the performance of the model by increasing the variance explained by approximately 3.5% and by reducing the RMSE by 0.5 kt. These improvements in the model are statistically significant at the 95% level. While the above results are based on 5-day mean SODA ocean reanalysis data, a similar analysis performed using EN4 monthly mean data gives consistent results, illustrating the robustness of the improvement. Although the results presented so far are based on 36-h intensity forecasts, we also carried out similar analyses for the 12-h forecast interval to provide hints on the applicability of $T_{dy}$ for other forecast periods. For 12-h intensity forecasts, replacing SST with $T_{dy}$ improves the performance of the model by increasing the variance explained by approximately 1.8% and reducing the RMSE by 0.15 kt. The reduction in the magnitude of the improvement for the 12-h forecast period when compared to the 36-h forecast period is in line with the understanding that the ocean's memory causes it to play an increasingly important role as the length of the forecast period increases (DeMaria and Kaplan 1994b, 1999). These changes, significant at the 95% level, show that the use of $T_{dy}$ can also improve the model at other forecast intervals.

## 4. Discussion

We have shown that the use of $T_{dy}$ can enhance the performance of the SHIPS framework significantly. The improvement mainly stems from the ability of $T_{dy}$ to account for upper-ocean stratification and its impact on hurricanes more accurately. The results from our study call for a better representation of hurricane–ocean interactions in SHIPS through the inclusion of $T_{dy}$ with the potential to improve hurricane intensity forecasts. The data needed to compute $T_{dy}$ include the current state of the storm and the subsurface ocean stratification, information that is already available in SHIPS. Since the subsurface temperature structure can be readily estimated using satellite sea surface temperature and altimetry (Shay and Brewster 2010; Pun et al. 2016), the $T_{dy}$ was computed with only temperature to show that improvements can be made to the model using the existing framework. However, there are a few regions where the salinity stratification could be important in the Atlantic, such as the Amazon outflow region (Balaguru et al. 2012a). Effects of upper-ocean salinity could potentially be included in near–real time through data from Argo floats (Roemmich et al. 2009) or satellite sea surface salinity (Grodsky et al. 2012). The impact of salinity on hurricane intensification is an area of active research (Balaguru et al. 2012a; Grodsky et al. 2012; Foltz and Balaguru 2016; Balaguru et al. 2016) and further efforts are needed in this regard. Finally, a few studies have shown that the use of nonlinear approaches in statistical modeling of hurricane intensity changes may improve the predictive skill (Baik and Hwang 1998; Lin et al. 2017). Future work to improve the SHIPS framework should take the application of such methods into consideration.

*Acknowledgments.* KB and DRJ were partially supported by the Department of Homeland Security (DHS) National Protection and Programs Directorate, Office of Cyber and Infrastructure Analysis. GRF was supported by NOAA's Climate Program Office and base funds to NOAA/AOML. LRL and SMH were supported by the Department of Energy (DOE)/Office of Science/Biological and Environmental Research's Regional and Global Climate Modeling Program. The Pacific Northwest National Laboratory (PNNL) is operated for DOE by Battelle Memorial Institute under Contract DE-AC05-76RL01830.

## REFERENCES

Baik, J.-J., and H.-S. Hwang, 1998: Tropical cyclone intensity prediction using regression method and neural network. *J. Meteor. Soc. Japan*, **76**, 711–717, https://doi.org/10.2151/jmsj1965.76.5_711.

Balaguru, K., P. Chang, R. Saravanan, and C. Jang, 2012a: The barrier layer of the Atlantic warmpool: Formation mechanism and influence on the mean climate. *Tellus*, **64A**, 18162, https://doi.org/10.3402/tellusa.v64i0.18162.

——, ——, ——, L. R. Leung, Z. Xu, M. Li, and J.-S. Hsieh, 2012b: Ocean barrier layers effect on tropical cyclone intensification. *Proc. Natl. Acad. Sci. USA*, **109**, 14 343–14 347, https://doi.org/10.1073/pnas.1201364109.

——, G. R. Foltz, L. R. Leung, E. D. Asaro, K. A. Emanuel, H. Liu, and S. E. Zedler, 2015: Dynamic potential intensity: An improved representation of the ocean's impact on tropical cyclones. *Geophys. Res. Lett.*, **42**, 6739–6746, https://doi.org/10.1002/2015GL064822.

——, ——, ——, and K. A. Emanuel, 2016: Global warming-induced upper-ocean freshening and the intensification of super typhoons. *Nat. Commun.*, **7**, 13670, https://doi.org/10.1038/ncomms13670.

Bender, M. A., and I. Ginis, 2000: Real-case simulations of hurricane–ocean interaction using a high-resolution coupled model: Effects on hurricane intensity. *Mon. Wea. Rev.*, **128**, 917–946, https://doi.org/10.1175/1520-0493(2000)128<0917:RCSOHO>2.0.CO;2.

Carton, J. A., and B. S. Giese, 2008: A reanalysis of ocean climate using Simple Ocean Data Assimilation (SODA). *Mon. Wea. Rev.*, **136**, 2999–3017, https://doi.org/10.1175/2007MWR1978.1.

D'Asaro, E. A., T. B. Sanford, P. P. Niiler, and E. J. Terrill, 2007: Cold wake of Hurricane Frances. *Geophys. Res. Lett.*, **34**, L15609, https://doi.org/10.1029/2007GL030160.

DeMaria, M., and J. Kaplan, 1994a: Sea surface temperature and the maximum intensity of Atlantic tropical cyclones. *J. Climate*, **7**, 1324–1334, https://doi.org/10.1175/1520-0442(1994)007<1324:SSTATM>2.0.CO;2.

——, and ——, 1994b: A statistical hurricane intensity prediction scheme (SHIPS) for the Atlantic basin. *Wea. Forecasting*, **9**, 209–220, https://doi.org/10.1175/1520-0434(1994)009<0209:ASHIPS>2.0.CO;2.

——, and ——, 1999: An updated Statistical Hurricane Intensity Prediction Scheme (SHIPS) for the Atlantic and eastern North Pacific basins. *Wea. Forecasting*, **14**, 326–337, https://doi.org/10.1175/1520-0434(1999)014<0326:AUSHIP>2.0.CO;2.

——, M. Mainelli, L. K. Shay, J. A. Knaff, and J. Kaplan, 2005: Further improvements to the Statistical Hurricane Intensity Prediction Scheme (SHIPS). *Wea. Forecasting*, **20**, 531–543, https://doi.org/10.1175/WAF862.1.

——, C. R. Sampson, J. A. Knaff, and K. D. Musgrave, 2014: Is tropical cyclone intensity guidance improving? *Bull. Amer. Meteor. Soc.*, **95**, 387–398, https://doi.org/10.1175/BAMS-D-12-00240.1.

Emanuel, K. A., 1986: An air–sea interaction theory for tropical cyclones. Part I: Steady-state maintenance. *J. Atmos. Sci.*, **43**, 585–605, https://doi.org/10.1175/1520-0469(1986)043<0585:AASITF>2.0.CO;2.

——, 1999: Thermodynamic control of hurricane intensity. *Nature*, **401**, 665–669, https://doi.org/10.1038/44326.

——, 2003: Tropical cyclones. *Annu. Rev. Earth Planet. Sci.*, **31**, 75–104, https://doi.org/10.1146/annurev.earth.31.100901.141259.

Foltz, G. R., and K. Balaguru, 2016: Prolonged El Niño conditions in 2014–2015 and the rapid intensification of Hurricane Patricia in the eastern Pacific. *Geophys. Res. Lett.*, **43**, 10 347–10 355, https://doi.org/10.1002/2016GL070274.

Gao, S., W. Zhang, J. Liu, I.-I. Lin, L. S. Chiu, and K. Cao, 2016: Improvements in typhoon intensity change classification by incorporating an ocean coupling potential intensity index into decision trees. *Wea. Forecasting*, **31**, 95–106, https://doi.org/10.1175/WAF-D-15-0062.1.

Goni, G. J., and J. A. Trinanes, 2003: Ocean thermal structure monitoring could aid in the intensity forecast of tropical cyclones. *Eos, Trans. Amer. Geophys. Union*, **84**, 573–578, https://doi.org/10.1029/2003EO510001.

Good, S. A., M. J. Martin, and N. A. Rayner, 2013: EN4: Quality controlled ocean temperature and salinity profiles and monthly objective analyses with uncertainty estimates. *J. Geophys. Res. Oceans*, **118**, 6704–6716, https://doi.org/10.1002/2013JC009067.

Grodsky, S. A., and Coauthors, 2012: Haline hurricane wake in the Amazon/Orinoco plume: AQUARIUS/SACD and SMOS observations. *Geophys. Res. Lett.*, **39**, L20603, https://doi.org/10.1029/2012GL053335.

Kanamitsu, M., W. Ebisuzaki, J. Woollen, S.-K. Yang, J. Hnilo, M. Fiorino, and G. Potter, 2002: NCEP–DOE AMIP-II reanalysis (R-2). *Bull. Amer. Meteor. Soc.*, **83**, 1631–1643, https://doi.org/10.1175/BAMS-83-11-1631.

Landsea, C., J. Franklin, and J. Beven, 2015: The revised Atlantic hurricane database (HURDAT2). NOAA/NWS, 6 pp., http://www.nhc.noaa.gov/data/hurdat/hurdat2-format-atlantic.pdf.

Leipper, D. F., and D. Volgenau, 1972: Hurricane heat potential of the Gulf of Mexico. *J. Phys. Oceanogr.*, **2**, 218–224, https://doi.org/10.1175/1520-0485(1972)002<0218:HHPOTG>2.0.CO;2.

Lin, I.-I., C.-C. Wu, K. A. Emanuel, I.-H. Lee, C.-R. Wu, and I.-F. Pun, 2005: The interaction of Supertyphoon Maemi (2003) with a warm ocean eddy. *Mon. Wea. Rev.*, **133**, 2635–2649, https://doi.org/10.1175/MWR3005.1.

——, and Coauthors, 2013: An ocean coupling potential intensity index for tropical cyclones. *Geophys. Res. Lett.*, **40**, 1878–1882, https://doi.org/10.1002/grl.50091.

Lin, N., R. Jing, Y. Wang, E. Yonekura, J. Fan, and L. Xue, 2017: A statistical investigation of the dependence of tropical cyclone intensity change on the surrounding environment. *Mon. Wea. Rev.*, **145**, 2813–2831, https://doi.org/10.1175/MWR-D-16-0368.1.

Lloyd, I. D., and G. A. Vecchi, 2011: Observational evidence for oceanic controls on hurricane intensity. *J. Climate*, **24**, 1138–1153, https://doi.org/10.1175/2010JCLI3763.1.

Mainelli, M., M. DeMaria, L. K. Shay, and G. Goni, 2008: Application of oceanic heat content estimation to operational forecasting of recent Atlantic category 5 hurricanes. *Wea. Forecasting*, **23**, 3–16, https://doi.org/10.1175/2007WAF2006111.1.

Pielke, R. A., Jr., J. Gratz, C. W. Landsea, D. Collins, M. A. Saunders, and R. Musulin, 2008: Normalized hurricane damage in the United States: 1900–2005. *Nat. Hazards Rev.*, **9**, 29–42, https://doi.org/10.1061/(ASCE)1527-6988(2008)9:1(29).

Price, J. F., 1981: Upper ocean response to a hurricane. *J. Phys. Oceanogr.*, **11**, 153–175, https://doi.org/10.1175/1520-0485(1981)011<0153:UORTAH>2.0.CO;2.

——, 2009: Metrics of hurricane–ocean interaction: Vertically-integrated or vertically-averaged ocean temperature? *Ocean Sci.*, **5**, 351–368, https://doi.org/10.5194/os-5-351-2009.

Pun, I.-F., J. F. Price, and S. R. Jayne, 2016: Satellite-derived ocean thermal structure for the North Atlantic hurricane season. *Mon. Wea. Rev.*, **144**, 877–896, https://doi.org/10.1175/MWR-D-15-0275.1.

Rappaport, E. N., J.-G. Jiing, C. W. Landsea, S. T. Murillo, and J. L. Franklin, 2012: The Joint Hurricane Test Bed: Its first decade of tropical cyclone research-to-operations activities reviewed. *Bull. Amer. Meteor. Soc.*, **93**, 371–380, https://doi.org/10.1175/BAMS-D-11-00037.1.

Roemmich, D., and Coauthors, 2009: The Argo Program: Observing the global ocean with profiling floats. *Oceanography*, **22** (2), 34–43, https://doi.org/10.5670/oceanog.2009.36.

Shay, L. K., and J. K. Brewster, 2010: Oceanic heat content variability in the eastern Pacific Ocean for hurricane intensity forecasting. *Mon. Wea. Rev.*, **138**, 2110–2131, https://doi.org/10.1175/2010MWR3189.1.

Stewart, S. R., 2017: Tropical cyclone report: Hurricane Matthew (AL142016) 28 September–9 October 2016. National Hurricane Center, https://www.nhc.noaa.gov/data/tcr/index.php?season=2016&basin=atl.